Research Square

Preprints are preliminary reports that have not undergone peer review.
They should not be considered conclusive, used to inform clinical practice,
or referenced by the media as validated information.

Magnetically reusable and well-dispersed nanoparticles for oxygen detection in water

Huahua Cui
Southern University of Science and Technology
Shanshan Wu
Southern University of Science and Technology
Lei Wang
Southern University of Science and Technology
Xiangzhong Sun
Southern University of Science and Technology
He Zhang
Southern University of Science and Technology
Mengyu Deng (dengmengyu_88@163.com)
Southern University of Science and Technology https://orcid.org/0000-0001-9203-4846
Yanqing Tian
Southern University of Science and Technology

Research Article

Keywords: magnetic, nanosensor, dissolved oxygen (DO), Escherichia coli

Posted Date: November 10th, 2021

DOI: https://doi.org/10.21203/rs.3.rs-1033265/v1

License: This work is licensed under a Creative Commons Attribution 4.0 International License.
Read Full License

Abstract

In this study, we aimed to synthesize magnetically well-dispersed nanosensors for detecting dissolved oxygen (DO) in water, and explore their biological applications. Firstly, we synthesized two kinds of magnetic nanoparticle with average sizes of approximately 82 nm by one-step emulsion polymerization: polystyrene magnetic nanoparticles (Fe_3O_4@Os1-PS) and polymethylmethacrylate magnetic nanoparticles (Fe_3O_4@Os1-PMMA). Both types of nanoparticle present good dispersibility and fluorescence stability. The nanoparticles could be used as oxygen sensors that exhibited a high DO-sensitivity response in the range 0-39.30 mg/L, with a strong linear relationship. The nanoparticles have good magnetic properties, and so they could be recycled by magnet for further use. Recovered Fe_3O_4@Os1-PS still presented high stability after continued use in oxygen sensing for one month. Furthermore, Fe_3O_4@Os1-PS was employed for detecting the bacterial oxygen consumption of Escherichia coli (E-coli) to monitor the metabolism of bacteria. The results show that Fe_3O_4@Os1-PS provide high biocompatibility and non-toxicity. Polystyrene magnetic nanoparticles therefore present significant potential for application in biological oxygen sensing.

1. Introduction

Dissolved oxygen (DO) plays a critical role in regulating multiple processes involved in complex biological systems [1–5]. Meanwhile, hypoxia usually leads to illness. Therefore, DO sensing is important for the diagnosis of certain diseases [6–8], and is usually realized by employing three methods: the Winkler titration method [9], the Clark electrochemistry method [10], and the optical method [11]. Among these, the optical method, which uses fluorescence sensors, is applied widely because of its non-invasive action on bacteria and tissues, high sensitivity, and real-time results [12].

Various oxygen probes that employ platinum/palladium porphyrinsas such as polyfluorence (PFO) [13], oligofluorene [14], and other emitters [15–17] are available to detect dissolved oxygen. Most of these are hydrophobic [18, 19], and difficult to apply in biological fields. Although some hydrophobic probes can be modified to increase solubility, their quantum yield is rather low [20, 21]. Porphyrin compounds are usually used in probes for DO sensors because of their high quantum yields and long excitation times [22–24].

To enable biological applications, scientists have explored various approaches, including the generation of nanoparticles with the assistance of polymers [25, 26]. Polymer materials for the connecting probe mainly include polymer nanoparticles, micelle polymers, and polymer films. Micelle polymers composed of multi-armed polymers may exhibit various morphologies and assemblies. However, micelle polymers sensors present various disadvantages, such as a long period of toxicity in vivo, and the difficulty of synthesizing micelle [27, 28]. Polymer films are unstable sensors when used to detect dissolved oxygen, although they are highly sensitive [29, 30]. Polymer nanoparticles with specific surface areas, mechanical properties, and higher dissolved-oxygen permeability, have gained considerable research attention, where the properties of polymer spheres largely depend on the polymer material employed [31, 32].

Although polyspheres with dissolved oxygen-sensitive probes have been reported in the literature, most of these are prone to agglomeration or precipitation, and have particular difficulty in forming a stable dispersion and solution system in water [33, 34]. Magnetical nanoparticles (NPs) are increasingly important in many biomedical applications, such as drug delivery, hyperthermia treatment, and magnetic resonance imaging (MRI) contrast enhancement [35, 36]. Otherwise, nanoparticles with magnetic properties can be recycled using magnetic separation.

In this paper, we synthesized two new kinds of nanoparticle using the incorporation of magnetic spheres and oxygen sensors, which employed PMMA and PS as the matrix. These two new nanoparticles named Fe_3O_4@Os1-PS and Fe_3O_4@Os1-PMMA were used for detecting DO. Both nanoparticle types exhibited good dispersity by optimizing and regulating amount of surfactants, while their non-toxicity indicates their potential for application in DO detection in biosystems such as bacteria or cells.

2. Experimental

2.1. Materials and reagents

Sodium dodecyl benzene sulfonate (SDBS) and ferric acetylacetonate $Fe(acac)_3$ were purchased from Energy Chemical (Shanghai, China). Styrene was purchased from Sinopharm Chemical Reagent Co., Ltd (Shanghai, China). Prior to use, the polymerization inhibitor in the styrene was removed using 10 % NaOH solution. Polyvinylpyrrolidone (PVP, K30), methyl methacrylate, oleic acid, oleylamine, and benzyl ether were purchased from Aladdin Industrial Corporation (Beijing, China). 1,2-hexadecanediol was purchased from Chemical Industry Co., Ltd (Tokyo, Japan). Ammonium persulfate was purchased from Lingfeng Chemical Reagent Co., Ltd (Shanghai, China), which served as an initiator of the redox polymerization of styrene and methyl methacrylate. 5-(4-methacryloxyethoxycarbonyl phenyl)-10,15,20-triphenyl-porphyrin (Os1) was synthesized according to reported procedures [15].

2.2. Instruments

Fe_3O_4@Os1-PS and Fe_3O_4@Os1-PMMA were separated by an ultra centrifuge (MAX-XP). Apparent morphologies were characterized using a scanning electron microscope (SEM, MIRA3 TESCAN) and a transmission electron microscope (TEM, Tecnai G2 F20 S-TWIN (200 kV) and HT7700). A PerkinElmer fluorescence spectrofluorophotometer was used for the fluorescence measurements. Dynamic light scattering (DLS) (Nano ZS, Malvern, UK) was used to measure the particle diameters. A vibrating sample magnetometer (VSM, JDAW-2000C&D) was employed to measure the hysteresis loop for Fe_3O_4 and Fe_3O_4@Os1-PS. Plate Reader (BioTek Cytation 3, Winooski, VT, USA) was used to measure bacteria respiration for Escherichia coli (E-coli). Dissolved oxygen and nitrogen gases were mixed at various concentrations using gas flow meters. All measurements were performed at room temperature (25 ℃ ± 5 ℃).

2.3. Preparation of Fe_3O_4 nanoparticles

Superparamagnetic Fe_3O_4 nanoparticles were synthesized according to the following approach [35]: $Fe(acac)_3$ (2 mmol, 0.7063 g), 1,2-hexadecanediol (10 mmol, 2.5845 g), oleic acid (6 mmol, 1.6948 g), oleylamine (6 mmol, 1.6049 g), and benzyl ether (20 mL) were mixed together, and further heated to 200 °C for 3 h under a nitrogen atmosphere. The product was then precipitated with ethanol and dispersed into 1.66 mL of hexane after centrifugation. The product was then placed in a refrigerator at −4 °C for further use.

2.4. Preparation of Fe_3O_4@Os1-PS and Fe_3O_4@Os1-PMMA

Fe_3O_4@Os1-PS was synthesized via the emulsifier polymerization of styrene and Os1 initiated by ammonium persulfate (APS): Firstly, 12 mg of SDBS and 40 mg of PVP solution were mixed and dissolved in 10 mL of water. Then, 400 μL of the above Fe_3O_4 dispersion solution, 0.2766 g styrene, and 2 mg Os1 dissolved in 200 μL of ethanol were added to the mixture. After ultrasonication, the suspension was degassed with nitrogen. To initiate polymerization, 0.0066 g of APS was added and stirred at a speed of 400 rpm for 5 h at 60°C with the protection of nitrogen gas. Finally,The resulting obtained magnetic nanoparticles were separated by centrifugation at 30000 rpm for 30 minutes. After washing twice with distilled water, 1 mg of magnetic nanoparticles was redispersed in 4 mL of distilled water for the detection of dissolved oxygen.

The synthetization method for the Fe_3O_4@Os1-PMMA nanoparticles is listed in supporting information, which is similar to the above methods with only the replacement of an equal amount of styrene with methyl methacrylate.

2.5. Sensor performance of dissolved oxygen

To investigate the sensing property of dissolved oxygen, the emission spectra excited at a wavelength of 405 nm under different dissolved oxygen in aqueous solutions were recorded at room temperature. Different ratios of DO were regulated by introducing mixtures of N_2 and O_2 into the solution using a cuvette and a pair of mass-flow controllers. The results for DO were analyzed quantitatively based on fluorescence intensities at 660 nm.

2.6. Detection of E. coli respirations and the toxicity of Fe_3O_4@Os1-PS for E.coli

E. coli were revived and cultivated in a liquid Lysogeny Broth (LB) medium at 37°C with shaking at 200 rpm for one night. The bacteria density of *E. coli* was estimated by measuring the optical density at 600 nm, which is linearly proportional to *E. coli* density when OD600 is in the range of 0.1 to 1.0. A value of 1 indicated a bacteria density of 5.0×10^8 colony-forming unit per milliliter (CFU/mL), based on the calibrations of the UV–vis spectrophotometer. The *E. coli* respiration and toxicity of Fe_3O_4@Os1-PS nanoparticles were analyzed using the plate reader. 100 μL of OD 0.025 bacteria densities of *E. coli* mixed with different concentrations of Fe_3O_4@Os1-PS were placed in 96 well plates to test toxicity. 100 μL of

different bacteria densities mixed with the concentration of 1 mg/4 ml of Fe_3O_4@Os1-PS were placed in 96 well plates to test oxygen respiration.

3. Results And Discussion

The magnetic Fe_3O_4 nanoparticles were synthesized according to the method described in the literature [35]. Transmission electron microscope (TEM) images (**Fig. S1a**) showed that the Fe_3O_4 nanoparticles were uniform in size with a diameter of approximately 4-8 nm. Moreover, a clear lattice structure is shown, which indicates that it has single-crystal properties that were further demonstrated through X-ray diffraction characterization (XRD in **Fig. S1b**). All diffraction peaks for Fe_3O_4 can be indexed to the [220], [311], [400], [422], [511], and [440] planes, which is consistent with the standard values of Fe_3O_4 according to the references of JCPDS card no. JCPDS 19-0629 [33, 37–38]. The VSM measurements (**Fig. S1c**) showed that the saturation magnetization (Sm) of ferric oxide was 44.8 emu/g, and the remanence and coercivity were zero, which may be related to its small particle size.

Furthermore, a magnetic nanosensor of Fe_3O_4@Os1-PS was prepared through emulsifier polymerization with an oxygen probe Os1, polymeric monomer (styrene), and magnetic Fe_3O_4 nanoparticles, as shown in Fig. 1. The magnetic nanosensor of Fe_3O_4@Os1-PMMA was adopted using the same synthetization method as in the case of Fe_3O_4@Os1-PS, by changing the styrene for methyl methacrylate, as shown in **Fig. S2**.

The nanoparticles have gained sizes of 50–100 nm after 5 hours under the reaction with protection of nitrogen. In order to know the sizes and morphologies of two types of nanoparticles, transmission electron microscope (TEM) and scanning electron microscope (SEM) were detected as they are the important means to demonstrate. TEM and SEM images for Fe_3O_4@Os1-PS and Fe_3O_4@Os1-PMMA are shown in Fig. 2. As shown in the TEM images of Fe_3O_4@Os1-PS (Fig. 2a) and Fe_3O_4@Os1-PMMA (Fig. 2b), it is evident that the Fe_3O_4 nanoparticles were wrapped in nanoparticles polymerized with styrene or methyl methacrylate as monomers, respectively. From Fig. 2c **and** Fig. 2d, both of these nanoparticles had diameter sizes of approximately 80 nm which can also be proved by the characterization of Dynamic lighting scattering (DLS). DLS (**Fig. S3a** and **Fig. S3b**) showed excellent dispersibility with low PDI, with 0.198 for Fe_3O_4@Os1-PS and 0.202 for Fe_3O_4@Os1-PMMA.

To study the oxygen-sensing properties of Fe_3O_4@Os1-PS and Fe_3O_4@Os1-PMMA in aqueous solutions, the emission spectra under different dissolved oxygen were recorded at room temperature. Dissolved oxygen was controlled by introducing different ratios of N_2 and O_2 into the solution within a cuvette, using a pair of mass-flow controllers. We typically allowed 180 s between the changes of the N_2 and O_2 gas mixtures to ensure a new equilibrium. The solution was excited at a wavelength of 405 nm, and maximum emission was monitored at 660 nm. After using 405-nm light to continuously excite Fe_3O_4@Os1-PS and Fe_3O_4@Os1-PMMA for 30 minutes, the intensities of their maximum emissions at 660 remained almost unchanged (**Fig. S4**), suggesting that these two new kinds of oxygen sensor are

particularly stable. It was observed that emission intensities of Fe_3O_4@Os1-PS (Fig. 3a) and Fe_3O_4@Os1-PMMA (Fig. 3b) at 660 nm (ascribed to Os1) decreased with increasing O_2 partial pressure from 0 % atm to 100 % atm. The emission ratios (I_0/I) and oxygen concentrations showed a linear relationship, following the Stern-Volmer Eq. (1).

$I_0/I=1+Ksv\ [PO_2]$ Eq. (1)

where I_0 and I are the steady-state luminescence signals at 660 nm, measured under nitrogen and under different O_2 partial pressures, respectively. K_{SV} is the Stern-Volmer quenching constant, and PO_2 denotes the O_2 partial pressures. As shown in Fig. 3c, the linear response to oxygen indicates a uniform distribution of the oxygen probes in the PS and PMMA matrix. The sensitivity of the oxygen sensor with nanoparticles is found to be 4.86-fold for Fe_3O_4@Os1-PS and 2.68-fold for Fe_3O_4@Os1-PMMA. Fe_3O_4@Os1-PS presented higher sensitivity for sensing. To explore whether the sensors of Fe_3O_4@Os1-PS can be reusable for detectiong dissolved oxygen (DO) when they were conserved for some time and redispersed in water, we conducted the extra experiments for the detection of oxygen sensitivity. Interestively, even after a month, Fe_3O_4@Os1-PS almost retained the same oxygen-detection sensitivity (**Fig. S5**), indicating that the sensor remained highly stable when redispersed in solution after a long time. Based on the advantages of fluorescence stability and reusable for the detection of dissolved oxygen (DO). Therefore, Fe_3O_4@Os1-PS was attempted to chosen as the exbacteriaent sensor for oxygen in the following experiment.

The magnetism characterization for Fe_3O_4@Os1-PS was performed using a vibrating sample magnetometer (VSM) at room temperature. VSM measurements showed that Fe_3O_4@Os1-PS could be used as a magnetic material because it presents a saturation magnetization (Sm) of 4.59 emu/g (Fig. 4a) which was decreased compared to the pure Fe_3O_4 nanoparticles due to the fact that small amounts of Fe_3O_4 was wrapped into the nanoparticles of Fe_3O_4@Os1-PS. Although the saturation magnetization (Sm) value of Fe_3O_4@Os1-PS has decreased increasingly, this nanoparticles can be quickly separated by less than 5 s by an external magnetic field. The magnetic nanoparticles may also be recycled using magnets for further use (Fig. 4b).

For biostudies, it is important to determine the toxicity assay for a new material. In this research, *E. coli* was cultured in LB broth at 37°C, with shaking at 200 rpm for 12 h. We incubated the same *E. coli* density (OD 0.025) in the multi-well plate with different concentrations of Fe_3O_4@Os1-PS nanoparticles. Blank 1 was the control test without the sensing nanoparticles, and blank 2 was the control test without E.coli. Absorbance was monitored at a wavelength of 600 nm (OD_{600}) using a plate reader. As shown in Fig. 5a, the time-dependent OD_{600} of *E. coli* was not influenced by Fe_3O_4@Os1-PS concentration, suggesting the non-toxicity and biocompatibility of the nanosensors.

Bacteria respiration is a key process for bacteria metabolism. Bacteria at a higher concentration can consume dissolved oxygen more rapidly. Bacteria were gradually diluted with LB broth to OD_{600} of 0.1,

0.05, 0.025 and 0.0125. Then 100 μL of the above-mentioned bacteria densities were mixed with 0.025mg/ml of Fe_3O_4@Os1-PS and placed in 96 well plates to test oxygen respiration, and the same volume of LB broth without bacteria was set as the blank control. To prevent the exchange of oxygen in the media with air, 100 μL of mineral oil was used to seal the well. For an excitation of 405 nm, emission intensity changes at a wavelength of 660 nm were recorded for the oxygen probe during bacteria growth. It was observed that the intensity of the oxygen probes' emission increased much faster at higher bacteria densities, indicating that the oxygen was consumed much faster at these higher densities (Fig. 5b). After the dissolved oxygen in the medium was completely consumed, the fluorescence intensity did not change further. A slight decrease in the fluorescence intensities at an early stage of the experiments was observed because of the temperature effect[34]. Together, these data showed that the nanosensors could detect the respiration of bacteria, and thus the metabolism of bacteria.

4. Conclusion

In this paper, we first synthesized two new types of magnetical nanoparticle, named Fe_3O_4@Os1-PS and Fe_3O_4@Os1-PMMA, which employed PS and PMMA as a matrix, respectively. Both nanoparticles exhibited good dispersity and fluorescence stability. Fe_3O_4@Os1-PS provided high sensitivity in terms of dissolved oxygen detection, and retained almost the same oxygen sensitivity even after a month. The sensors presented good biocompatibility and were successfully applied to the real-time monitoring of bacteria oxygen respiration for *E. coli*. It is expected that these new types of magnetic nanoparticles could be applied as oxygen sensors in related research into bacteria growth and metabolism.

Declarations

Author Contributions

Methodology: Cui H. and Wu S.; Formal analysis and investigation: Cui H., Wang L., Sun X. and Zhang H.; Writing—original draft preparation: Cui H.; Writing—review and editing: Cui H., Wu S and Deng M.; Supervision: Wu S., Deng M. and Tian Y.

Funding: This work was supported by National Natural Science Foundation of China (21574061, 21774054), Shenzhen Fundamental Research Programs (JCYJ20190809120013254), and Guangdong Industry Polytechnic (KJ2019-003 and 150124910).

Data Availability: The data and material are available within the manuscript.

Ethical Approval: Not applicable.

Consent to Participate: Not applicable.

Consent for Publication: Not applicable.

Conflict of interest: The authors have no competing interests to declare that are relevant to the content of this article.

References

1. Zhang P, Guo JH, Wang Y, Pang WQ (2002) Incorporation of luminescent tris(bipyridine) ruthenium (II) complex in mesoporous silica spheres and their spectroscopic and dissolved oxygen-sensing properties. Mater. Lett. 53:400–405. https://doi.org/10.1016/S0167-577X(01)00514-6
2. Chu CS, Sung TW, Lo YL (2013) Enhanced optical dissolved oxygen sensing property based on Pt(II) complex and metal-coated silica nanoparticles embedded in sol–gel matrix. Sensors Actuat. B, Chem. 185:287–292. https://doi.org/10.1016/j.snb.2013.05.011
3. Papkovsky DB, Dmitriev RI (2013) Biological detection by optical dissolved oxygen sensing. Chem. Soc. Rev. 42:8700–8732. https://doi.org/10.1039/C3CS60131E
4. Lu SS, Xu W, Zhang JL, Chen YY, Xie L, Yao QH, Jiang YQ, Wang YR, Chen X (2016) Facile synthesis of a ratiometric dissolved oxygen nanosensor for bacteriaular imaging. Biosens. Bioelectron. 86:176–184. https://doi.org/10.1016/j.bios.2016.06.050
5. Morris RL, Schmidt TM (2013) Shallow Breathing: Bacterial Life at Low O_2. Nature Reviews Microbiology. 11: 205-212. https://doi.org/10.1038/nrmicro2970
6. Wang XH, Peng HS, Yang L, You FT, Teng F, Hou LL, Wolfbeis OS (2014) Targetable Phosphorescent Oxygen Nanosensors for the assessment of tumor mitochondrial dysfunction by Monitoring the Respiratory Activity. Angewandte Chemie, 126:12679-12683. https://doi.org/10.1002/ange.201405048
7. Will Y, J Hynes, Ogurtsov VI, Papkovsky DB (2006) Analysis of Mitochondrial Function Using Phosphorescent Oxygen-Sensitive Probes. Nature Protocols, 1:2563-2572. https://doi.org/10.1038/nprot.2006.351
8. Christofk HR, Vander Heiden MG, Harris MH, Ramanathan A, Gerszten RE, Wei R, Fleming MD, Schrebier SL, Cantley LC (2008) The M2 Splice Isoform of Pyruvate Kinase is Important for Cancer Metabolism and Tumour Growth. Nature, 452:230-233. https://doi.org/10.1038/nature06734
9. Winkler LW (1953) Die Bestimmung des im Wasser gelosten Sauerstoffee, Ber. Dtsch. Chem. Ges. 21: 2843-2855.
10. Clark LC, Wolf JrR, Granger D, Taylor Z (1953) Continuous recording of blood oxygen tensions by polarography. J. Appl. Physiol 6:189-193. https://doi.org/10.1152/jappl.1953.6.3.189
11. Su FY, Alam R, Mei Q, Tian YQ, Youngbull C, Johnson RH, Meldrum DR (2012) Nanostructured oxygen sensor - using mibacteriaes to incorporate a hydrophobic platinum porphyrin, PLoS One 7: e33390.
12. Im SH, Khali GE, Callis J, Ahn BH, Gouterman M, Xia Y (2005) Synthesis of polystyrene beads loaded with dual luminophors for self-referenced dissolved oxygen sensing. Talanta 67:492–497. https://doi.org/10.1016/j.talanta.2005.06.046

13. Xu W, Lu SS, Xu MX, Jiang YQ, Wang YR, Chen X (2016) Simultaneous imaging of intrabacteriaular pH and O_2 using functionalized semiconducting polymer dots. J. Mater. Chem. B 4*:* 292–298. https://doi.org/10.1039/C5TB02071A
14. Lu HG, Jin YG, Tian YQ, Zhang WW, Holla MR, Meldrum DR (2011) New ratio metric optical oxygen and pH dual sensors with threee mission colors for measuring photo synthetic activity in cyano bacteria. J. Mater. Chem. C 21:19293-19301. https://doi.org/10.1039/C1JM13754A
15. Zhou XS, Su FY, Tian YQ, Johnson RH, Meldrum DR (2011) Platinum (II) porphyrin containing thermoresponsive poly(N-isopropylacrylamide) copolymer as fluorescence dual oxygen and temperature sensor. Actuators B Chem 159:135-141. https://doi.org/10.1016/j.snb.2011.06.061
16. Zhang CF, Ingram J, Schiff S, Xu J, Xiao M (2011) Probing oxygen consumption in epileptic brain slices with QDs-based FRET *sensors.* SPIEOPTO 7974:22-27. https://doi.org/10.1117/12.876341
17. Wang YD, Wolfbeis OS (2014) Optical methods for sensing and imaging oxygen: materials, spectroscopies and applications. Chem. Soc. Rev 43:3666-3761. https://doi.org/10.1039/C4CS00039K
18. Carraway ER, Demas JN, Degraff BA, Bacon JR (1991) Photo physics and photochemistry of oxygen sensors based on luminescent transition-metal complexes. Anal. Chem 63:337–342. https://doi.org/10.1021/ac00004a007
19. Mills A, Lepre A (1997) Controlling the response characteristics of luminescent porphyrin plastic film sensors for oxygen. Anal. Chem 69:4653–4659. https://doi.org/10.1021/ac970430g
20. O'Donovan C, Hynes J, Yashunski D, Papkovsky DB (2005) Phosphorescent oxygen-sensitive materials for biological applications. J. Mater. Chem 15:2946–2951. https://doi.org/10.1039/B501748C
21. O'Riordan TC, Fitzgerald K, Ponomarev GV, Mackrill J, Hynes J, Taylor C, Papkovsky DB (2007) Sensing intracellular oxygen using near-infrared phosphorescent probes and live-cell fluorescence imaging. Am. J. Physiol. Regul. Integr. Comp. Physiol 292:R1613–R1620. https://doi.org/10.1152/ajpregu.00707.2006
22. Shi JY, Zhou YF, Jiang JP, Pan TT, Mei ZP, Wen JX, Yang C, Wang ZJ, Tian YQ (2019) Multi-arm polymers prepared by atom transfer radical polymerization (ATRP) and their electrospun films as oxygen sensors and pressure sensitive paints. European Polymer Journal 112:214–221. https://doi.org/10.1016/j.eurpolymj.2019.01.008
23. Li XL, Roussakis E, Cascales JP, Marks HL, Witthauer L, Evers M, Mansteinband D, Evans C (2021) Optimization of bright, highly flexible, and humidity insensitive porphyrin-based oxygen-sensing materials. J. Mater. Chem. C 9: 7555–7567. https://doi.org/10.1039/D1TC01164B
24. Vinogradov SA, Lo LW, Jenkins WT, Evans SM, Koch C, Wilson DF (1996) Noninvasive Imaging of The Distribution in Oxygen in Tissue In Vivo Using Near-Infrared Phosphors. Biophysical Journal 70:1609-1617. https://doi.org/10.1016/S0006-3495(96)79764-3
25. Inglev R, Møller E, Højgaard J, Bang O, Janting J (2021) Optimization of All Polymer Optical Fiber Oxygen Sensors with Antenna Dyes and Improved Solvent Selection Using Hansen Solubility

Parameters. Sensors 21:5. https://doi.org/10.3390/s21010005

26. Lee WWS, K WW, Li XM, Leung YB, Chan CH, Chan KH (1993) Halogenated Platinum Porphyrins as Sensing Materials for Luminescence-Based Oxygen Sensors. J. Mater. Chem 3:1031-1035. https://doi.org/10.1039/JM9930301031
27. Qiao Y, Pan TT, Li JZ, Yang C, Wen JX, Zhong K, Wu SS, Su FY, Tian YQ (2019) Extracellular Oxygen Sensors Based on PtTFPP and Four-Arm Block Copolymers. Appl. Sci 9:4404. https://doi.org/10.3390/app9204404
28. Li JZ, Qiao Y, Pan TT, Zhong K, Wen JX, Wu SS, Su FY, Tian YQ (2018) Amphiphilic Fluorine-Containing Block Copolymers as Carriers for Hydrophobic PtTFPP for Dissolved Oxygen Sensing, Cell Respiration Monitoring and In Vivo Hypoxia Imaging with High Quantum Efficiency and Long Life time. Sensors 18:3752. https://doi.org/10.3390/s18113752
29. Mao YY, Zhao Q, Wu JC, Pan TT, Zhou BP, Tian YQ (2017) A highly sensitive and fast-responding oxygen sensor based on POSS-containing hybrid copolymer films. J. Mater. Chem. C 5:135–141. https://doi.org/10.1039/C7TC03606J
30. Zhang HL, Zhang ZG (2020) Ratiometric Sensor Based on PtOEP-C6/Poly (St-TFEMA) Film for Automatic Dissolved Oxygen Content Detection. Sensors 20:6175. https://doi.org/10.3390/s20216175
31. Deng MY, Qiao Y, Liu C, Wang ZJ, Shi JY, Pan TT, Mao YY, Me ZP, Huang F, Tian YQ (2019). Tricolorcore/shell polymeric ratiometric nanosensors for intracellular glucose and oxygen dual sensing. Sensors & Actuators: B. Chemical 286:437–444. https://doi.org/10.1016/j.snb.2019.01.163
32. Zhang K, Zhang HL, Lia WJ, Tian YQ, Lia S, Zhao JP, Li Y (2016) PtOEP/Ps composite particles based on fluorescent sensor for dissolved oxygen detection. Mater. Lett 172:112–115. https://doi.org/10.1016/j.matlet.2016.02.119
33. Mao YY, Mei ZP, Liang LF, Zhou BP, Tian YQ (2018) Robust and magnetically recoverable dual-sensor particles: Real-time monitoring of glucose and dissolved oxygen. Sensors Actuat. B Chem *262:* 371–379. https://doi.org/10.1016/j.snb.2018.02.024
34. Liang LF, Li G, Mei ZP, Shi JY, Mao YY, Pan TT, Liao CZ, Zhang JB, Tian YQ (2018) Preparation and application of ratiometric polystyrene-based nanoparticles as oxygen sensors. Anal. Chim. Acta. 1030:194-201. https://doi.org/10.1016/j.aca.2018.05.017
35. Sun S, Zeng H (2002) Size-Controlled Synthesis of Magnetite Nanoparticles. J. Am. Chem. Soc. 124:8204-8205. https://doi.org/10.1021/ja026501x
36. Cheong S, Ferguson P, Feindel KW, Hermans LF, Callaghan PT, Meyer C, Slocombe A, Su CH, Cheng FY, Yeh CS, Ingham B, Toney MF, Tilley RD (2011) Simple synthesis and functionalization of iron nanoparticles for magnetic resonance imaging. *Angew. Chem. Int. Ed. 50:*4206–4209. https://doi.org/10.1002/ange.201100562
37. Xiao CW, Liu XJ, Mao SM, Zhang LJ, L J (2017) Sub-micron-sized polyethylenimine-modified polystyrene/Fe3O4/chitosan magnetic composites for the efficient and recyclable adsorption of Cu(II) ions. *Applied Surface Science.* 394:378–385. http://dx.doi.org/10.1016/j.apsusc.2016.10.116

38. Xu JS, Zhao C, Hu TY, Chen X, Cao YH (2021) Rapid preparation of size-tunable Fe_3O_4@SiO_2 nanoparticles to construct magnetically responsive photonic crystals. *J Nanopart Res.* 23:232. https://doi. org/10.1007/s11051-021-05342-x

Figures

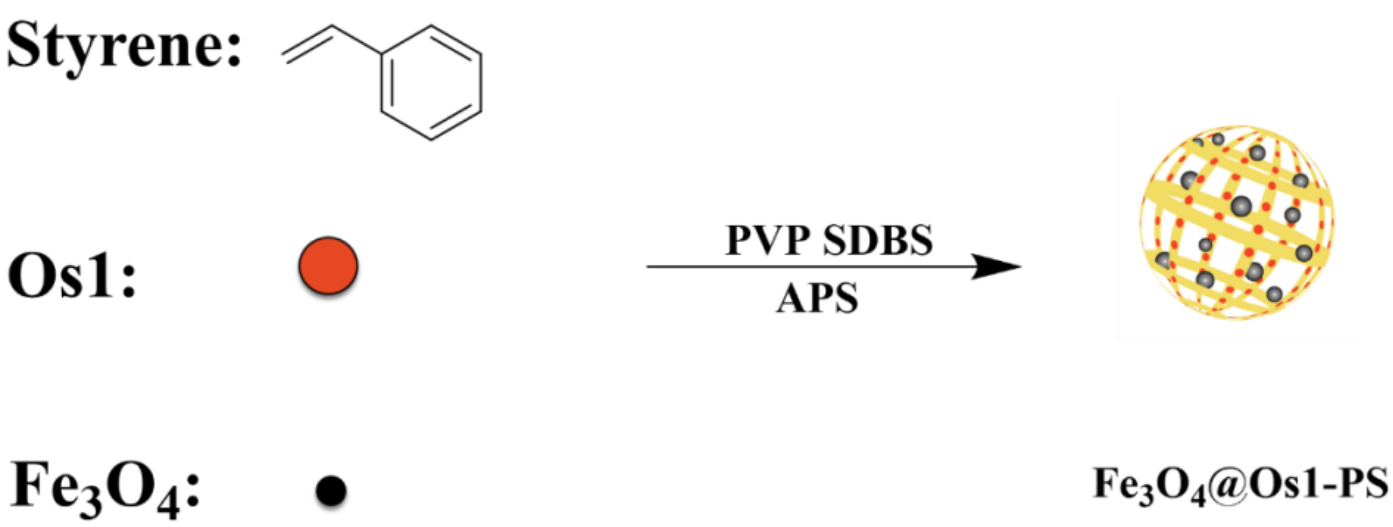

Figure 1

Simple schematic drawing of the preparation process for Fe3O4@Os1-PS nanosensors.

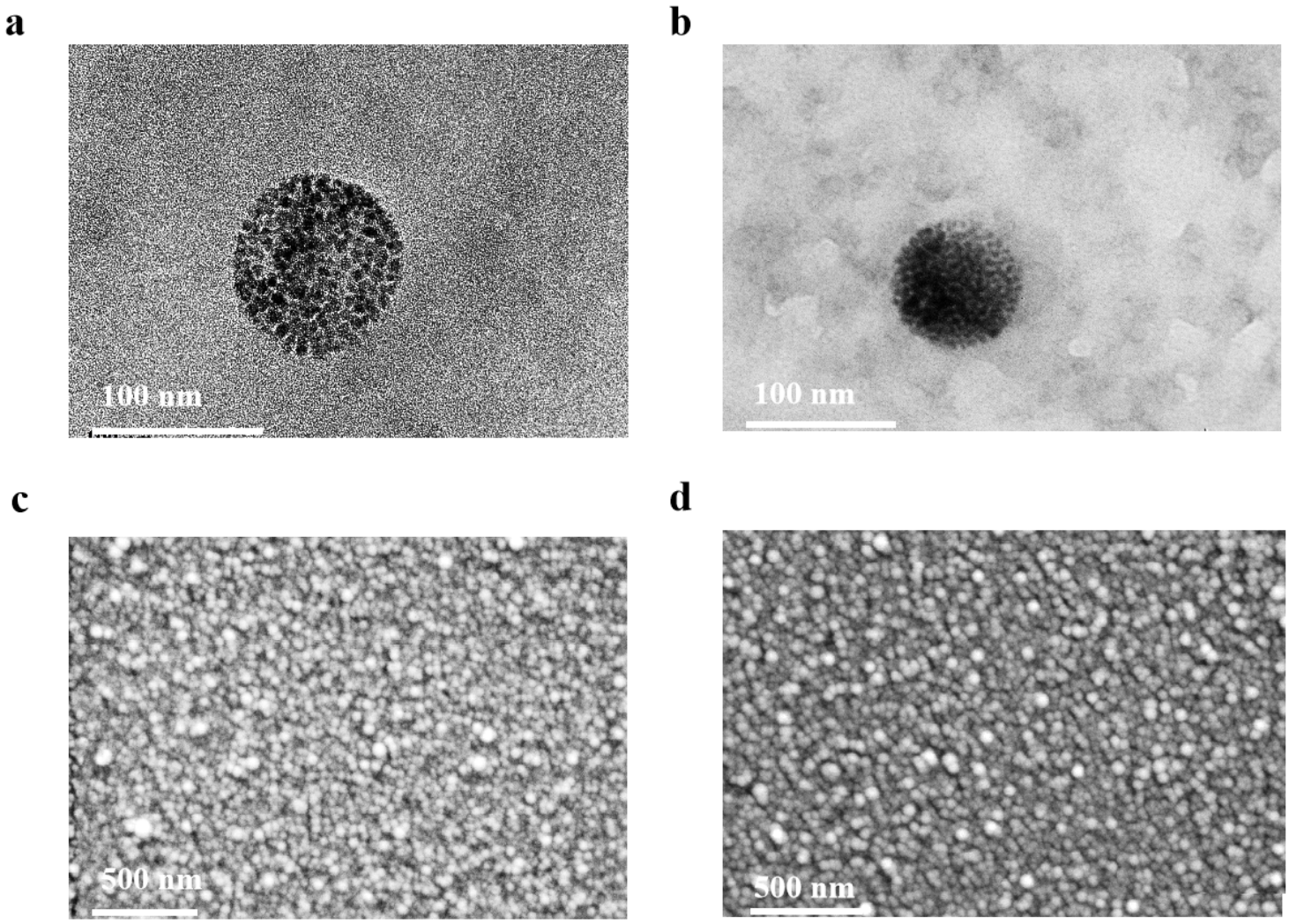

Figure 2

TEM images for a) Fe3O4@Os1-PS and b) Fe3O4@Os1-PMMA. SEM images for c) Fe3O4-Os1-PS and d) Fe3O4@Os1-PMMA.

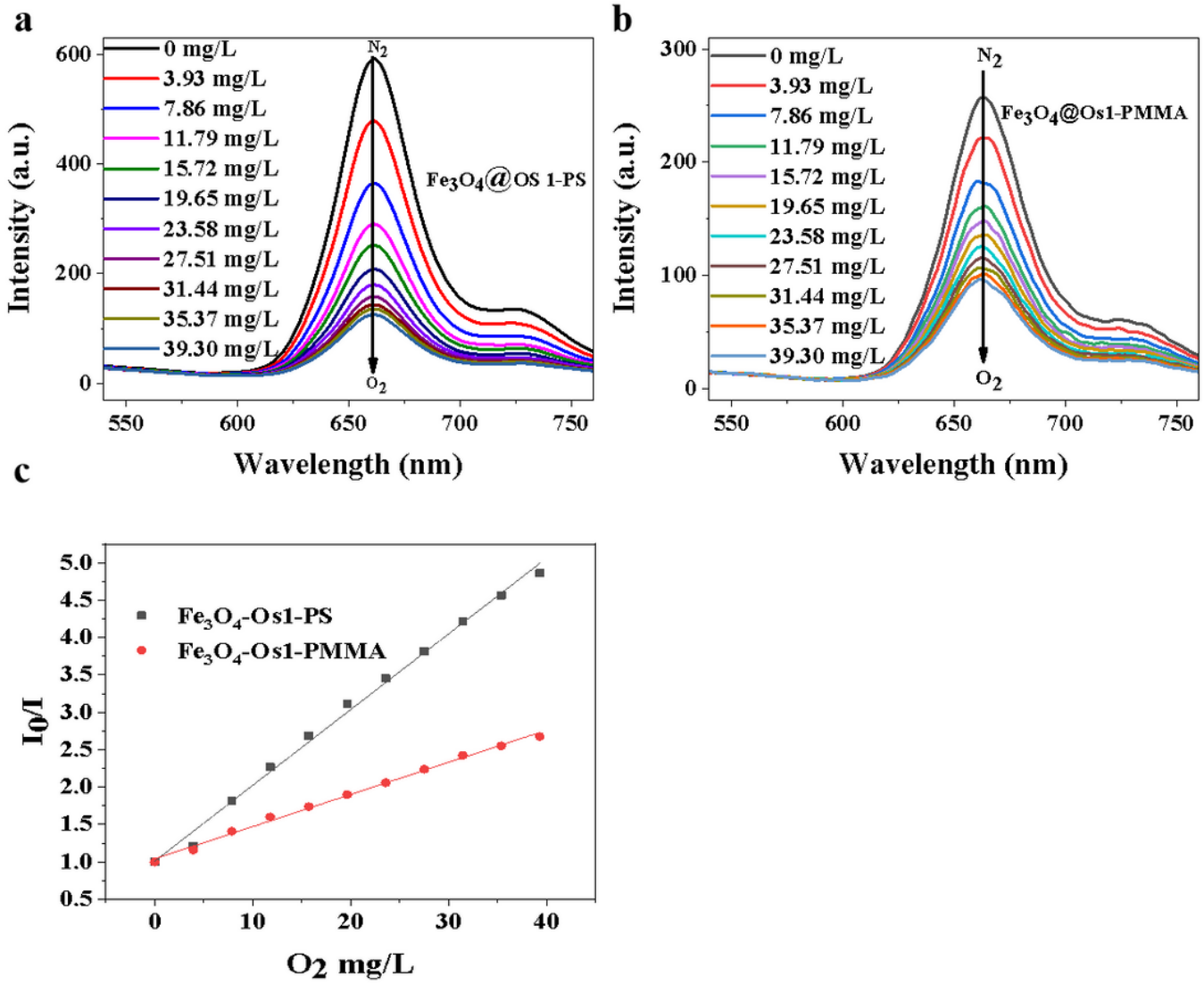

Figure 3

Dissolved oxygen sensing responses of a) Fe3O4@Os1-PS and b) Fe3O4@Os1-PMMA; c) Stern-Volmer plots of gaseous dissolved oxygen sensing for Fe3O4@Os1-PS and Fe3O4@Os1-PMMA.

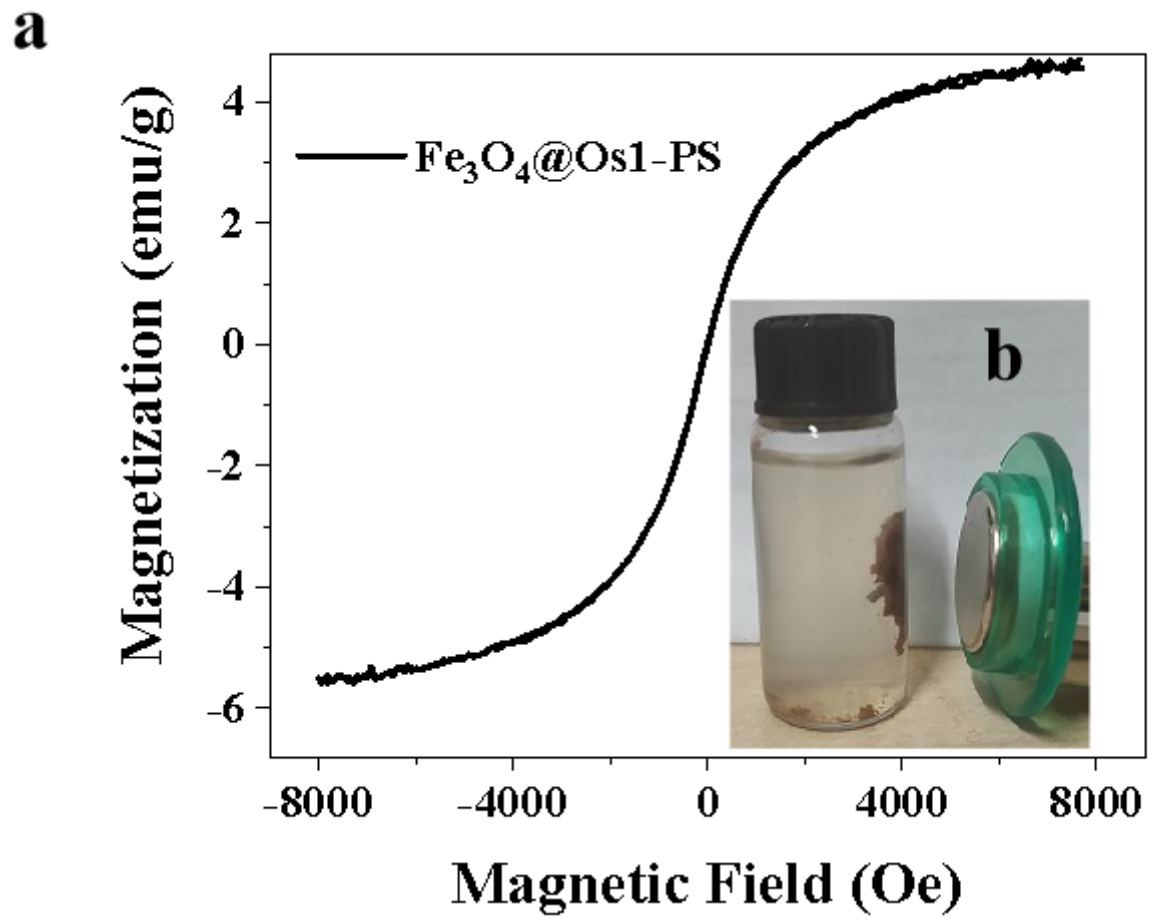

Figure 4

Magnetism characterization for Fe3O4@Os1-PS: a) VSM detection and b) a recycled Fe3O4@Os1-PS microsphere.

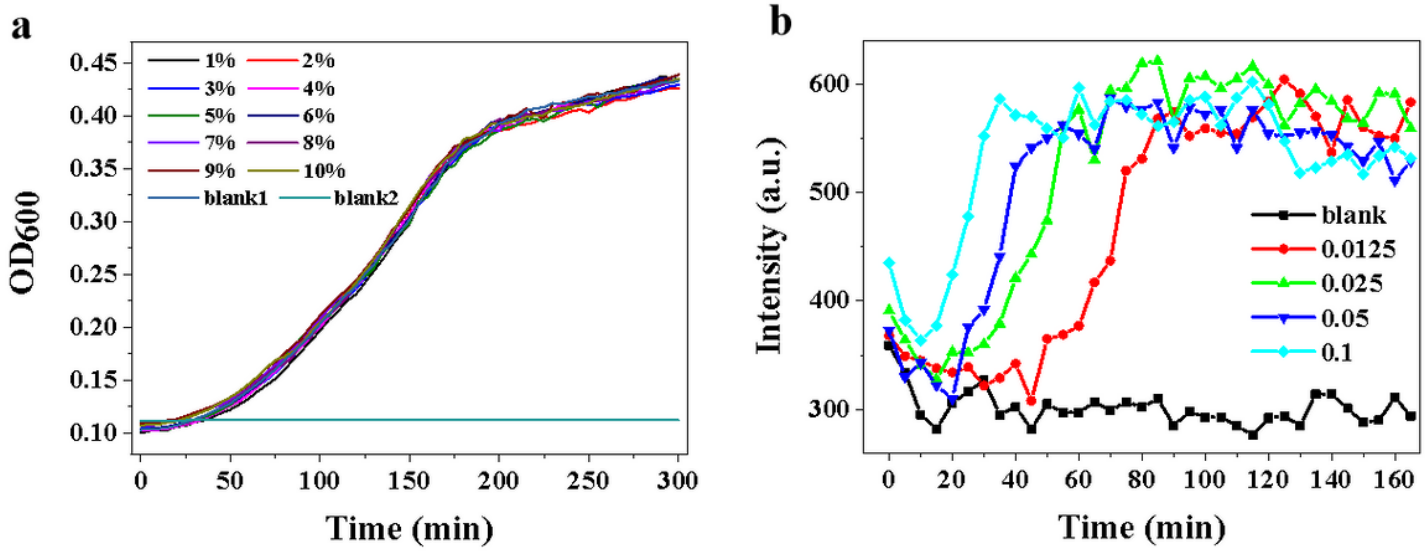

Figure 5

a) Bacteria toxicity test at different concentrations of Fe3O4@Os1-PS at 37 °C. Blank 1 indicates only 0.025 of E. coli in the media, without Fe3O4@Os1-PS nanoparticles. Blank 2 indicates the consequences without the presence of E.coli. b) Time-dependent emission intensity changes at a wavelength of 660 nm under excitation at 405 nm at different OD600 of 0.1, 0.05, 0.025, and 0.0125 of E. coli, and without nanosensors (named “blank”).

Supplementary Files

This is a list of supplementary files associated with this preprint. Click to download.

- si.docx